Available online at www.sciencedirect.com

ScienceDirect

Polymer 48 (2007) 5548–5555

polymer

www.elsevier.com/locate/polymer

Electropolymerization of 1,2-methylenedioxybenzene in 1-butyl-3-methylimidazolium hexafluorophosphate room temperature ionic liquid

Bin Dong [a,b], Liqiang Zheng [a,*], Jingkun Xu [b,*], Houting Liu [b], Shouzhi Pu [b]

[a] Key Laboratory of Colloid and Interface Chemistry (Shandong University), Ministry of Education, Jinan 250100, China
[b] Jiangxi Key Laboratory of Organic Chemistry, Jiangxi Science and Technology Normal University, Nanchang 330013, China

Received 29 May 2007; received in revised form 5 July 2007; accepted 16 July 2007
Available online 21 July 2007

Abstract

The electrochemical polymerization of 1,2-methylenedioxybenzene (MDOB) in a room temperature ionic liquid 1-butyl-3-methylimidazolium hexafluorophosphate ($BmimPF_6$) has been investigated. Its polymer poly(1,2-methylenedioxybenzene) (PMDOB) showed good redox activity and stability even in concentrated sulfuric acid. IR and ^1H NMR spectra confirmed that the polymerization occurred at the C_4 and C_5 positions on the benzene ring of MDOB, resulting in the main backbone of PMDOB similar to polyacetylene. In contrast to acetonitrile containing 0.1 mol/L Bu_4NBF_4, $BmimPF_6$ serves as both the growth medium and an electrolyte. Hence, enhanced electrochemical stability of PMDOB can be easily obtained on repetitive redox cycling. As-formed PMDOB represented good electrochromic properties from green grass to opalescent between doped and dedoped states. Scanning electron microscopic results demonstrated that smooth and compact PMDOB films composed of ordered nanostructures were obtained, implying their possible utilizations in ion-sieving films, ion-selective, and matrices for catalyst particles.

Keywords: Ionic liquid; Electrochemical polymerization; Poly(1,2-methylenedioxybenzene)

1. Introduction

Inherently conducting polymers (CPs), which exhibit numerous novel electrochemical and chemical properties, have extensive applications, such as supercapacitors, sensors and electrochromic devices. Among the CPs, polyacetylene is the prototype and was intensively investigated in the past [1]. In addition, considerable attention has been paid to polypyrrole (PPy), polythiophene (PTh), poly(*p*-phenylene) (PPP), and polyaniline (PANI). In particular the derivative of PTh, poly(3,4-ethylenedioxythiophene) (PEDOT) has developed into one of the most successful materials from both the practical and academic viewpoints [2]. However, the realization of practical CP electrochemical devices remains difficult because of poor environmental stability and short lifetimes when electrochemically cycling between oxidation and reduction states. These defects derive partly from the electrolytes used in the electrosyntheses of CPs, such as aqueous and organic electrolytes.

Ionic liquids (ILs), a class of organic molten electrolytes at or near ambient temperature, have been the focus of many scientific investigations because of their specific physical and chemical properties [3]. In recent years, ILs based on the 1-alkyl-3-methylimidazolium cation $[C_n\text{mim}]^+$ have attracted much interest. They have no significant vapor pressures, non-flammability, outstanding catalytic properties, stability at temperatures up to 300 °C or more, and are relatively inexpensive to manufacture. Therefore, ILs have attracted much attention as electrolytes [4] and solvent media for reactions and

---

* Corresponding authors. Tel.: +86 791 3805183; fax: +86 791 3826894.
E-mail addresses: lqzheng@sdu.edu.cn (L. Zheng), xujingkun@tsinghua.org.cn (J. Xu).

0032-3861/$ - see front matter © 2007 Elsevier Ltd. All rights reserved.
doi:10.1016/j.polymer.2007.07.038

extractions [5]. Furthermore, as electrolytes with wide potential windows and high ionic conductivity, the air and moisture stable ILs are expected to be peculiarly suitable medium for electropolymerization.

In fact, the electrosyntheses of PPy [6], PTh [7], PPP [8], PANI [9], and PEDOT [10] in different ILs such as 1-ethyl-3-methylimidazolium trifluoromethanesulfonate (EmimOTf), 1-butyl-3-methylimidazolium hexafluorophosphate ($BmimPF_6$), 1-butyl-3-methylimidazolium tetrafluoroborate ($BmimPF_4$), 1-hexyl-3-methylimidazolium tri(pentafluoroethyl)trifluorophosphate (HmimFAP), 1-ethylimidazolium trifluoroacetate (HeimTfa), and 1-ethyl-3-methylimidazolium bis((trifluoromethyl)sulfonyl)amide ($EmimTf_2N$), have been reported in the literature. As a result, use of ionic liquids as the growth medium leads to significantly altered film morphologies and improved electrochemical activities. However, to the best of our knowledge, there are very few reports on the electropolymerization of the alkylenedioxy-substituted benzene. Our group has reported the direct anodic oxidation of 1,2-methylenedioxybenzene (MDOB), one of the analogues of 3,4-alkylenedioxythiophene and 3,4-alkylenedioxypyrrole, in the traditional organic solvent acetonitrile containing 0.1 mol/L Bu_4NBF_4 [11]. The main advantage for this monomer is its cheap commercial price, which will be beneficial to the polymer application.

In this work, we present for the first time the electrochemical polymerization of MDOB in the hydrophobic ionic liquid $BmimPF_6$. In contrast to acetonitrile containing 0.1 mol/L Bu_4NBF_4, $BmimPF_6$ serves as both the growth medium and an electrolyte and delivers much milder chemical conditions. Compact PMDOB films were obtained and represented enhanced electrochemical stability and good electrochromic properties from green grass (doped) to opalescent (dedoped).

2. Experimental

2.1. Chemicals

$BmimPF_6$ was prepared according to the procedure reported by Dupont et al. [12]. Before use, $BmimPF_6$ was dried under a vacuum. MDOB (Acros Organics) was used directly without further purification; its concentration in $BmimPF_6$ was 0.28 mol/L. Concentrated sulfuric acid (98 wt%), 25 wt% ammonia (Jinan Chemical Reagent Co., Ltd.), and dimethyl sulfoxide (DMSO; Tianjin Bodi Chemicals Co., Ltd.) were analytical grade reagents and were used as received. Deuterium-substituted dimethyl sulfoxide (DMSO-d_6) was purchased from Beijing East Longshun Chemical Plant.

2.2. Electropolymerization

Electrochemical polymerizations and examinations were performed in a one-compartment cell by the use of model 263 potentiostat–galvanostat (EG&G Princeton Applied Research) under computer control at 10 °C. To obtain a sufficient amount of PMDOB for characterization, stainless steel sheets with surface areas of 10 and 12 cm^2 each were employed as the working and counter electrodes, respectively. Prior to each experiment, the electrodes were polished with abrasive paper (1500 mesh) and cleaned with water and acetone successively. The PMDOB films were grown potentiostatically and the amount was controlled by the integrated current passing through the cell. Then they were washed with acetonitrile to remove the ionic liquid remaining in the polymer films. Electrochemical measurements were carried out with a platinum wire (diameter 0.5 mm). A stainless steel wire (diameter 1 mm) served as the counter electrode and an Ag/AgCl electrode was used as the reference electrode. Its electrode potential was calibrated against a saturated calomel electrode and revealed sufficient stability during the experiment. The potentials mentioned in this paper refer to the Ag/AgCl electrode. All the measurements were carried out under a nitrogen atmosphere to avoid the effect of oxygen. For spectral analysis, PMDOB films were dedoped with 25 wt% ammonia for 3 days and then washed repeatedly with distilled water. Finally, they were dried in vacuum at 60 °C for 24 h.

2.3. Characterizations

Infrared (IR) spectra were recorded by using KBr pellets on the Bruker Vertex 70 FT-IR spectrometer. ^1H NMR spectra were recorded on a Bruker AV 400 NMR spectrometer, and DMSO-d_6 was used as the solvent. UV–vis spectra were taken by using a Perkin–Elmer Lamda 900 UV–vis–NIR spectrophotometer. The fluorescence spectra were determined with an F-4500 fluorescence spectrophotometer (Hitachi). The thermogravimetric (TG) and differential thermogravimetric (DTG) analyses were performed with a Netzsch TG209 thermal analyzer. Scanning electron microscopic (SEM) measurements were performed using a JEOL JSM-6360 LA scanning electron microscope. The fluorescence quantum efficiency (Φ) of PMDOB in solution was measured and calculated according to the well-known method given as:

$$\Phi = \frac{n^2 A_{\mathrm{ref}} I}{n_{\mathrm{ref}}^2 A I_{\mathrm{ref}}} \Phi_{\mathrm{ref}} \tag{1}$$

where ref denotes the reference, n is the refractive index of the solvent, A is the absorbance at the excitation wavelength, and I is the intensity of the emission spectrum. Here, we use anthracene in acetonitrile ($\Phi_{\mathrm{ref}} = 0.27$) as the reference [13]. It is worth mentioning that absorbance of the sample and the reference should be similar and small (<0.10) [14].

3. Results and discussion

3.1. Electrochemical syntheses of PMDOB films

Fig. 1 represents 20 successive cyclic voltammograms (CVs) in the course of electrochemical polymerization of MDOB in $BmimPF_6$. Such a CV is typical for the electropolymerization of CPs. From the first cycle, it is clearly seen that the oxidation onset of MDOB was initiated at about 1.24 V, which corresponded to the oxidation of MDOB to its radical cation, while there was an obvious reductive peak near

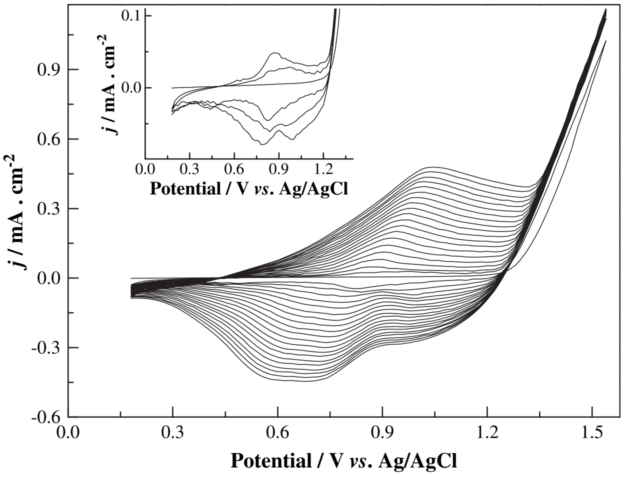

Fig. 1. Cyclic voltammograms of 0.28 mol/L MDOB in $BmimPF_6$. Scan rate: 100 mV/s. The inset shows an enlargement of the first three cycles.

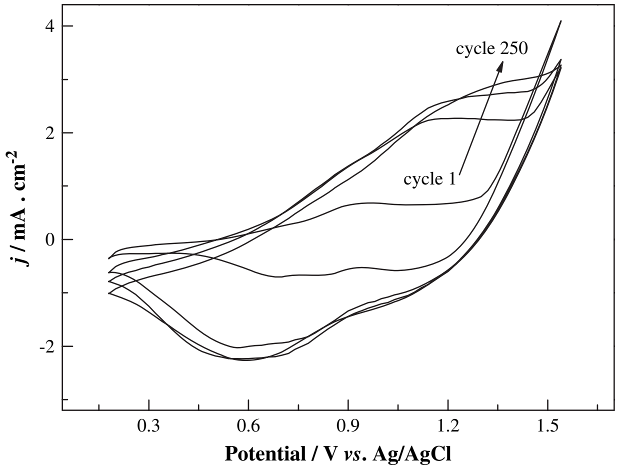

Fig. 2. Extended cyclic voltammograms of PMDOB films in monomer-free $BmimPF_6$ at a potential scan rate of 100 mV/s. Cycles 1, 50, 100, and 250 are presented. The film was synthesized electrochemically in $BmimPF_6$ at a constant applied potential of 1.54 V vs Ag/AgCl.

0.83 V. In the second cycle, an oxidation peak at 0.95 V appeared, and two reductive peaks were observed near 0.84 and 0.98 V, respectively. This pair of peaks may be assigned to the transformation from quinoid structure to aromatic state. Anodic and cathodic wave currents increased with increasing the potential scanning cycle, indicating that the amount of the polymer deposited on the electrode increased. The potential shift of the peak wave current implied the increase of the electrical resistance in the polymer and the overpotential needed to overcome the resistance [15]. The similar phenomenon was reported in the electropolymerization of this monomer in acetonitrile containing 0.1 mol/L Bu_4NBF_4 [11]. Although the electrodes as well as the scan rate were different, the larger increasing interval of the peak current densities indicated that the PMDOB film of higher quality was formed in $BmimPF_6$ than in acetonitrile. Visual inspection during the deposition of the polymer revealed that a baby blue film formed on the platinum electrode after the second cycle. On subsequent scans, the color gradually changed, and finally a green grass polymer film was obtained on the electrode surface. It is worth mentioning that the potential scanning range is much smaller than the electrochemical window of $BmimPF_6$ [3], and there was no deposit at all in the monomer-free $BmimPF_6$ solution.

3.2. Electrochemistry of PMDOB films

The electrochemical properties of PMDOB films prepared electrochemically from $BmimPF_6$ in monomer-free $BmimPF_6$ were determined, as shown in Fig. 2. At the first scan cycle, the redox waves were relatively weak, indicating as-formed PMDOB film with low doping level. As the CV scans proceeded, the current densities of the oxidation or reduction waves increased distinctly, indicating the increase of the doping level of the PMDOB film. After 100 CV scans, the current densities of the redox waves were almost constant and the PMDOB film represented enhanced electrochemical stability. Thus, these results demonstrated that as-formed PMDOB film was much less charged than it could be, and that the successive CV scanning is an effective technique for the further doping of the film. The analogous observation has been reported for some conducting polymers prepared in the traditional organic solvent [16].

The electrochemical behavior of as-formed PMDOB films was determined in monomer-free $BmimPF_6$ (Fig. 3A) and in concentrated sulfuric acid (Fig. 3B). As can be seen clearly, all the steady-state CVs represented broad anodic and cathodic peaks. This may be ascribed to the presence of coupling defects distributed statically, resulting in the wide distribution of the polymer chain length [17]. The peak current densities were proportional to the scanning rates (inset of Fig. 3A and B), indicating a redox couple fixing on the electrode. However, the redox processes are not controlled by diffusion. Furthermore, PMDOB films could be cycled repeatedly between the conducting (oxidized) and the insulating (neutral) states without decomposition even in concentrated sulfuric acid, implying the good redox activity and high structure stability of the polymer. The polymer films could be oxidized and reduced from 1.04 V (anodic peak potential, E_a) to 0.68 V (cathodic peak potential, E_c) in $BmimPF_6$, and from 0.62 V (E_a) to 0.49 V (E_c) in concentrated sulfuric acid. The difference between E_a and E_c related to the kinetics of the doping–dedoping reaction was equal to 0.36 V in $BmimPF_6$ and 0.13 V in concentrated sulfuric acid.

The lowest unoccupied molecular orbital (LUMO) and the highest occupied molecular orbital (HOMO) energy levels of PMDOB were determined from the onset of reduction and oxidation potentials, respectively, by assuming the energy level of ferrocene/ferrocenium (Fc) to be −4.8 eV below vacuum [18]. The empirical equations are as follows:

$$E_{\mathrm{LUMO}} = -e\left(E_{\mathrm{onset}}^{\mathrm{re}} + 4.8\right)\ \mathrm{V} \qquad (2)$$

$$E_{\mathrm{HOMO}} = -e\left(E_{\mathrm{onset}}^{\mathrm{ox}} + 4.8\right)\ \mathrm{V} \qquad (3)$$

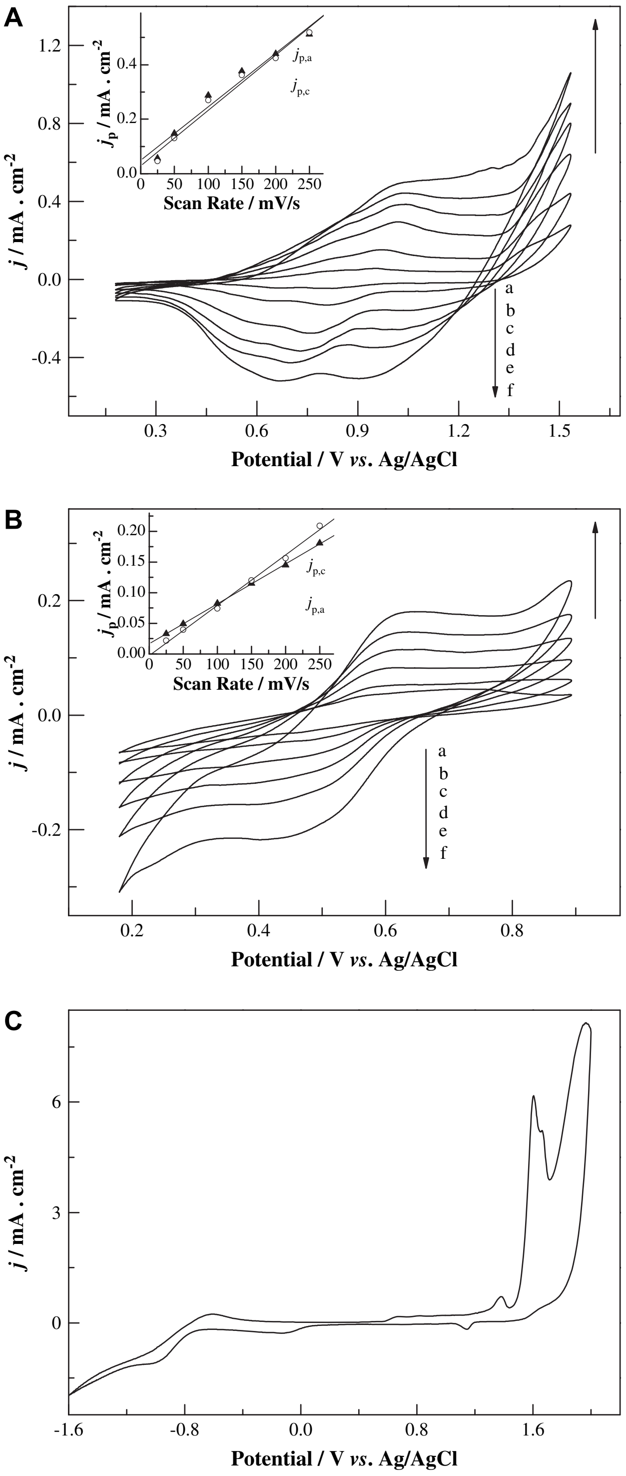

Fig. 3. Cyclic voltammograms of PMDOB films in pure $BmimPF_6$ (A) and concentrated sulfuric acid (B) at potential scan rates of 25 (a), 50 (b), 100 (c), 150 (d), 200 (e), and 250 (f) mV/s. (C) Cyclic voltammograms of PMDOB films in ACN containing 0.1 mol/L Bu_4NBF_4 at a potential scan rate of 50 mV/s. The films were synthesized electrochemically in $BmimPF_6$ at a constant applied potential of 1.54 V vs Ag/AgCl. Note: j, j_p, $j_{p,a}$, and $j_{p,c}$ are defined as the current density, the peak current densities, the anodic peak current densities, and the cathodic peak current densities, respectively.

As shown in Fig. 3C, E^{re}_{onset} and E^{ox}_{onset} of PMDOB in ACN containing 0.1 mol/L Bu_4NBF_4 were observed at −0.74 and +1.44 V vs Ag/AgCl, respectively, which correspond to an E_{LUMO} value of −4.06 eV and an E_{HOMO} value of −6.24 eV. Moreover, the electrochemical band gap (E^{ec}_g) was determined to be 2.18 eV ($E^{ec}_g = E_{LUMO} - E_{HOMO}$) [14]. Note that obtaining absolute LUMO and HOMO levels by electrochemical method is still under debate, and thus, these values should be considered as crude estimates.

3.3. Structural characterizations

During the potentiostatic deposition of PMDOB in $BmimPF_6$, the color of the electrolyte solution progressively changed to slight orange. This indicated that partly soluble oligomers formed and diffused away from the electrode into the solution during anodic oxidation. With the propagation of polymerization, the soluble oligomers became insoluble and deposited on the working electrode with elongation of the PMDOB main backbone chain. However, some oligomers still diffused into the solution, making the color of the solution darker. Doped and dedoped PMDOB electrosynthesized in $BmimPF_6$ can dissolve in strong polar organic solvent DMSO and the solution is orange in color. For characterization of the structure and properties of as-formed PMDOB, IR, ^{1}H NMR, UV–vis and fluorescence spectra were performed.

Fig. 4 illustrates the infrared spectra of the monomer MDOB (A) and doped PMDOB film (B) obtained potentiostatically from $BmimPF_6$. It can be clearly seen that there were evident changes between the monomer and the polymer. The strong and narrow peaks centered at 2891 and 1479 cm^{-1} in the monomer (Fig. 4A) were assigned to the stretching of $-CH_2-$ and the vibration of C–C in the aromatic ring, which were broader and shifted to 2902 and 1460 cm^{-1} in the polymer, respectively (Fig. 4B). The C–O–C asymmetry stretching of the monomer and polymer appeared at 936 and 938 cm^{-1}, respectively. These results indicated that the

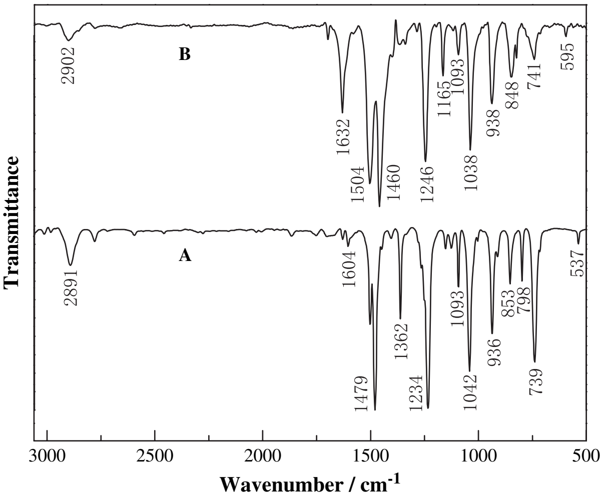

Fig. 4. FT-IR spectra of MDOB (A) and PMDOB (B) obtained potentiostatically at 1.54 V vs Ag/AgCl from $BmimPF_6$.

aromatic ring and the C–O–C band are very stable and still exist on the PMDOB backbone. Thus, the polymerization sites could not be at the C_3, C_6 or C_7 position (chemical structure in the inset of Fig. 5). The peaks of MDOB centered at 739 cm^{-1} and multiple peaks from 2000 to 1604 cm^{-1} were assigned to the 1,2-disubstituted aromatic ring (Fig. 4A). However, these peaks changed obviously in the spectrum of PMDOB (Fig. 4B); the double peaks appeared at 1632 and 1504 cm^{-1}, and a single peak was centered at 741 cm^{-1}, indicating a 1,2,4,5-substituted benzene ring (chemical structure in the inset of Fig. 5). This implied that the polymerization of MDOB may happen at the C_4 and C_5 positions.

To get deep insight into the polymer structure and the polymerization mechanism, the ^1H NMR spectra of the monomer MDOB (Fig. 5B and C) and the PMDOB film (Fig. 5A) obtained potentiostatically from $BmimPF_6$ were recorded. Three group peaks could be found in Fig. 5B: 5.96, 6.79–6.83, and 6.85–6.88 ppm, which were assigned to the protons at the C_7, $C_3(_6)$, and $C_4(_5)$ positions, respectively. Because of the spin–spin splitting between protons at C_3 and C_4 (or C_6 and C_5) positions, multiple peaks appeared as shown in Fig. 5C. However, in the spectrum of PMDOB, there was only one singlet at 8.14 ppm. There may be two coupling mechanisms of MDOB: at C_3 and C_6, or C_4 and C_5 positions. If the polymerization happened at C_3 and C_6 positions, the proton line would be a doublet. Therefore, this singlet proton peak could be assigned to the protons at C_3 or C_6 positions. These results indicated that the polymerization should happen at C_4 and C_5 positions, in good agreement with the IR results. The main backbone of PMDOB was similar to polyacetylene, one of the simplest CPs. Meanwhile, the chemical shift moving to lower field indicated the higher conjugation length on the polymer main backbone [11].

The UV–vis spectra of MDOB (A), doped PMDOB (B), and dedoped PMDOB (C) in DMSO are shown in Fig. 6. It can be seen that, similar to the monomer, the polymer also exhibited strong absorption at 280 nm and another wide absorption of the polymer appeared from 303 to 359 nm. Generally, the higher the wavelength of the absorption, the higher the conjugation length of the polymer [19]. Thus, the UV–vis spectra results confirmed the formation of a conjugated polymer. In addition, the spectra of the doped and dedoped PMDOB were essentially the same, which may be due to the automatic dedoping process of PMDOB in DMSO solution. The band gap of PMDOB obtained from the onset of the optical absorption spectra (E_g^{opt}) was roughly 3.31 eV ($E_g^{opt} = 1240/\lambda_{onset}$ (nm)) [14]. The difference between E_g^{opt} (3.31 eV) and E_g^{ec} (2.18 eV) may be due to the fact that the band gap generally depends on the determination method.

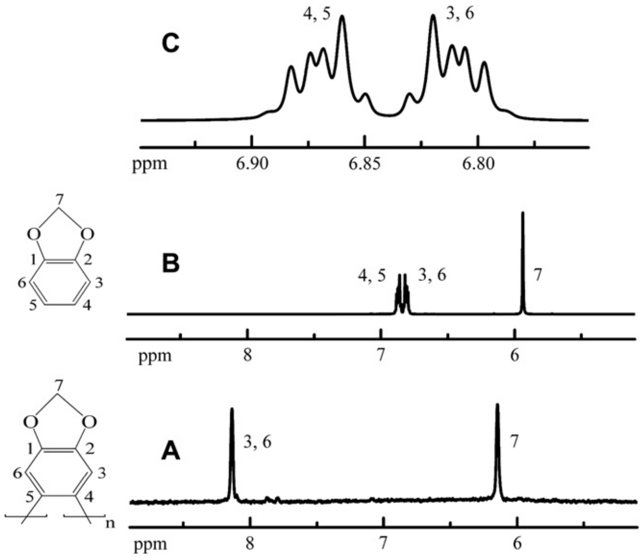

Fig. 5. ^1H NMR spectra of MDOB (B and C) and PMDOB (A) obtained potentiostatically at 1.54 V vs Ag/AgCl from $BmimPF_6$. Solvent: DMSO-d_6.

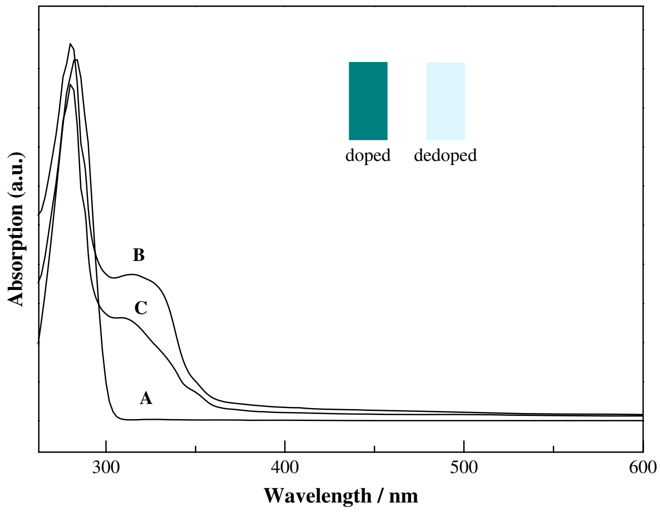

Fig. 6. UV–vis spectra of MDOB (A), doped PMDOB (B), and dedoped PMDOB (C) obtained potentiostatically at 1.54 V vs Ag/AgCl from $BmimPF_6$. Solvent: DMSO. Inset: Color of the doped and dedoped PMDOB films on ITO electrode.

On the other hand, the electrochromic stability of PMDOB on the platinum electrode in $BmimPF_6$ was not good. However, PMDOB films on ITO electrode represented good electrochromic properties between the doped and the dedoped states, from green grass to opalescent (inset of Fig. 6). This may be ascribed to the short conjugation length of PMDOB on the platinum electrode, in comparison with other popular conducting polymers together with the moving in/out of counterions during the doping and dedoping processes [11].

The fluorescence spectra of MDOB, doped and dedoped PMDOB prepared from $BmimPF_6$ were measured with DMSO as the solvent through the wavelength scans of emission, as shown in Fig. 7. The emission spectrum of MDOB has an obvious peak at 320 nm (Fig. 7A). On the other hand, the obvious emission peaks of doped and dedoped PMDOB (Fig. 7B and C) can be found at 388 and 408 nm. This indicated that there was a large red shift between the monomer and the polymer. This further proved the formation of the conjugated backbone of PMDOB, in accordance with the UV–vis and ^1H NMR spectral results. The slight

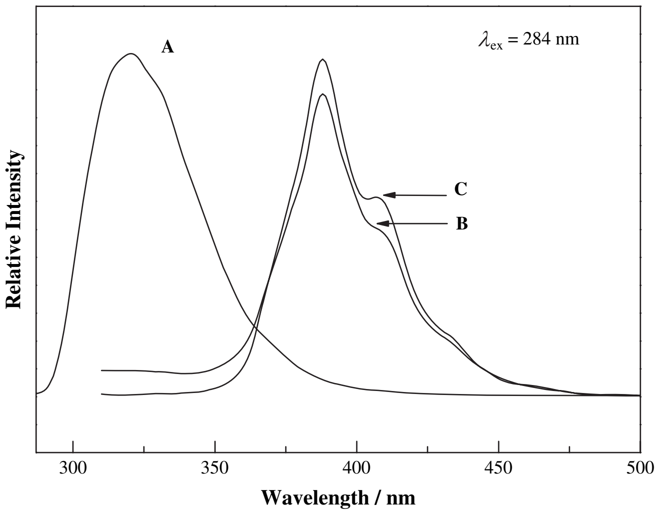

Fig. 7. Emission spectra of MDOB (A), doped PMDOB (B), and dedoped PMDOB (C) obtained potentiostatically at 1.54 V vs Ag/AgCl from $BmimPF_6$. Solvent: DMSO.

difference between doped and dedoped PMDOB may be the effect of counterion. The fluorescence quantum efficiency of as-formed PMDOB in DMSO was measured to be 0.091 according to Eq. (1). These results demonstrate that PMDOB is a blue light emitter, indicating some potential applications in organic optoelectronics.

3.4. Thermal analysis

The thermal stability of conducting polymers is very important for their potential application. To investigate the thermal stability of as-formed PMDOB prepared from $BmimPF_6$, the thermal analyses were performed under a nitrogen stream from 300 to 1058 K with a heating rate of 10 K/min. As seen in the thermogravimetric curve (Fig. 8A), the structure of the PMDOB main backbone chain was kept up to 598 K. There was a three-step loss of weight. The first one is slight from 300 to 598 K, up to 11.57%, resulting from evaporation of water or other moisture trapped in PMDOB [20]. The second one occurred from 598 to 707 K, up to 18.67%, which may be due to the degradation of the skeletal PMDOB backbone chain structure. The last one was about 15.59% from 707 to 1058 K, probably owing to the overflow of some oligomers decomposing from PMDOB with the increase of the temperature. From the differential thermogravimetric curve (Fig. 8B), it can be seen that the most rapid weight change rate of PMDOB occurred at 697.49 K. All these results indicated that the thermal stability of PMDOB prepared from $BmimPF_6$ was acceptable.

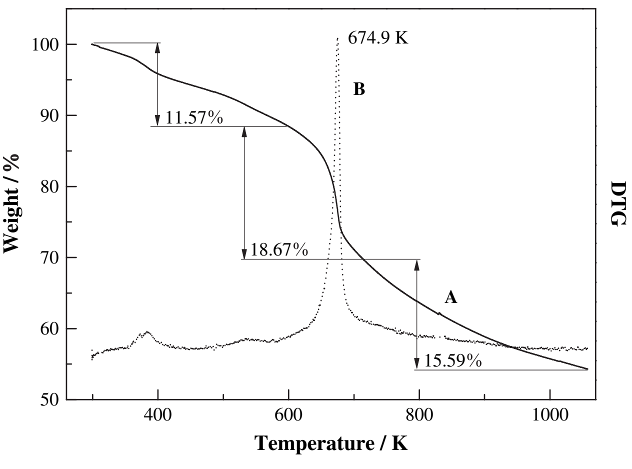

Fig. 8. TGA curves of doped PMDOB films obtained potentiostatically at 1.54 V vs Ag/AgCl from $BmimPF_6$.

3.5. Morphology

The surface morphology of PMDOB films deposited on the ITO electrode prepared from $BmimPF_6$ was observed by SEM (Fig. 9). The doped PMDOB film was very smooth and uniform (Fig. 9A). In Fig. 9B, the selected resolution of the SEM revealed that an ordered nanostructure with sizes of around 40 nm was recognizable, suggesting the easy access of electrolyte into the polymer surface [21]. The nanostructure is beneficial in improving conductivity and electron transfer capability [9]. After dedoping at a constant applied potential of −0.4 V, the surface of PMDOB film was still rather smooth (Fig. 9C). At a magnification of 15,000 (Fig. 9D), a slightly cracked structure was observed, which may be ascribed to the migration of counterion out of the polymer surface. In contrast to acetonitrile containing 0.1 mol/L Bu_4NBF_4 [11], $BmimPF_6$ serves as both the growth medium and an electrolyte, leading to the formation of compact PMDOB films. Therefore, they may have potential application in ion-sieving films, ion-selective electrodes, and matrices for hosting catalyst particles [22]. Moreover, $BmimPF_6$ delivers much milder chemical conditions than organic solvent acetonitrile. Usually, the production of nanomaterials through electrochemical method needs templates such as Al_2O_3 or polycarbonate or using a template-free method [23]. During the polymerization of MDOB in $BmimPF_6$, no templates or surfactants were used. Hence, the formation of PMDOB nanostructures should be a template-free approach. The ITO electrode acted as nucleation center and self-assembly occurred around these centers.

4. Conclusions

The conducting polymer PMDOB was electrochemically deposited by direct anodic oxidation of MDOB in air and moisture stable ionic liquid 1-butyl-3-methylimidazolium hexafluorophosphate ($BmimPF_6$). IR and ^1H NMR spectra determined that the main backbone of PMDOB was similar to polyacetylene. In contrast to acetonitrile containing 0.1 mol/L Bu_4NBF_4, $BmimPF_6$ serves as both the growth medium and an electrolyte and delivers much milder chemical conditions. Compact PMDOB films with nanostructures were obtained and represented enhanced electrochemical stability and good electrochromic properties from green grass (doped)

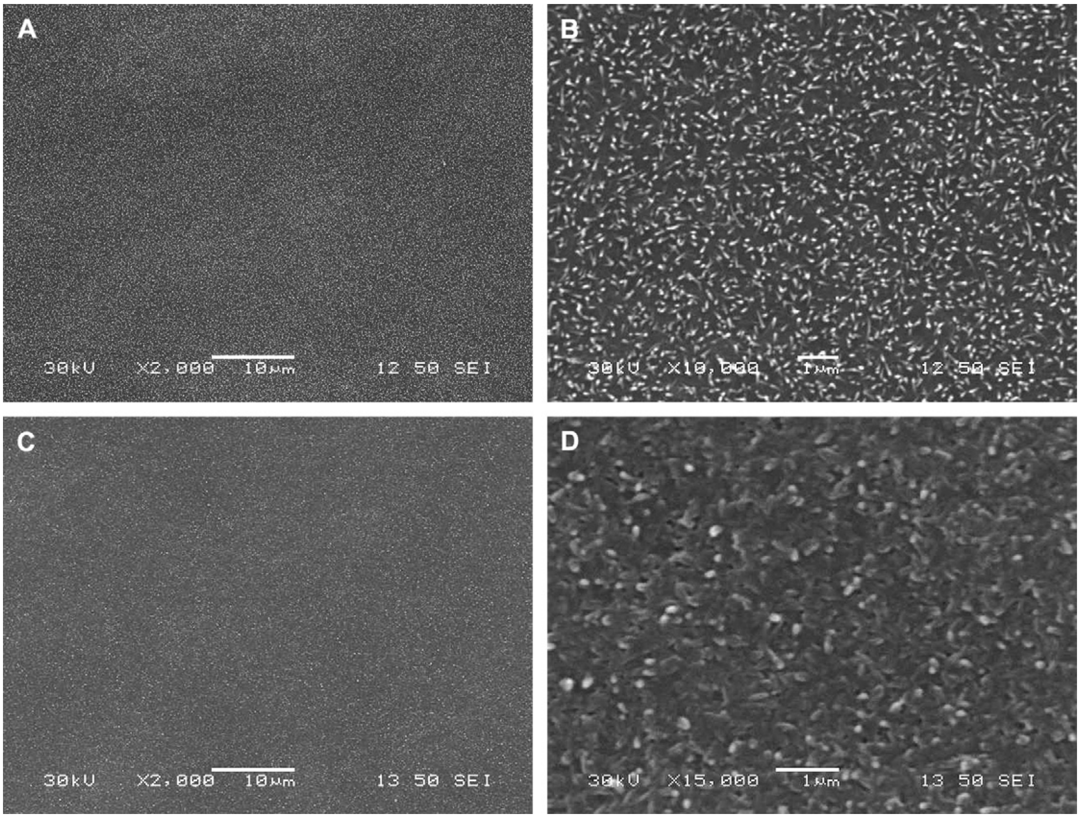

Fig. 9. SEM micrographs of PMDOB films on ITO electrode obtained potentiostatically at 1.54 V vs Ag/AgCl from $BmimPF_6$. A and B: doped; C and D: dedoped.

to opalescent (dedoped). The fluorescence spectra indicated that PMDOB was a blue light emitter, with the fluorescence quantum efficiency in DMSO of 0.091.

Acknowledgements

This work was supported by Natural Scientific Foundation of China (Grant Nos. 50663001 and 50472069), Ministry of Education (2007-207058) and the National Basic Research Program (2007CB808004, Z2004B02).

References

[1] Naarmann H. In: Kuzmany H, Mehring M, Roth S, editors. Properties of conjugated polymers. Heidelberg, New York: Springer; 1987.

[2] (a) Groenendaal L, Zotti G, Auber PH, Waybright SM, Reynold JR. Adv Mater 2003;15(11):855–79;
(b) Gao YY, Zhao L, Li C, Shi GQ. Polymer 2006;47(14):4953–8.

[3] (a) Robin DR, Kenneth RS. Science 2003;302:792–3;
(b) Li RX. Green solvent: synthesis and application of ionic liquids. Beijing: Chemistry Technology Press; 2004.

[4] (a) McEwen AB, Ngo HL, Lecompte K, Goldman JL. J Electrochem Soc 1999;146:1687;
(b) Nakajima H, Ohno H. Polymer 2005;46(25):11499–504.

[5] (a) Welton T. Chem Rev 1999;99(8):2071–84;
(b) Blanchard LA, Hancu A, Bechman EJ, Brennecke JF. Nature 1999; 399:28–9;
(c) Anthony JL, Maginn EJ, Brennecke JF. J Phys Chem B 2002;106(29): 7315–20.

[6] (a) Sekiguchi K, Atobe M, Fuchigami T. Electrochem Commun 2002;4(11):881–5;
(b) Sekiguchi K, Atobe M, Fuchigami T. J Electroanal Chem 2003;557: 1–7;
(c) Mazurkiewicz JH, Innis PC, Wallace GG, MacFarlane DR, Forsyth M. Synth Met 2003;135–136:31–2;
(d) Pringle JM, Efthimiadis J, Howlett PC, Efthimiadis J, MacFarlane DR, Chaplin AB, et al. Polymer 2004;45(5):1447–53.

[7] (a) Lu W, Fadeev AG, Qi BH, Smela E, Mattes BR, Ding J, et al. Science 2002;297:983–7;
(b) Pringle JM, Forsyth M, MacFarlane DR, Wagner K, Hall SB, Officer DL. Polymer 2005;46(7):2047–58.

[8] Zein El Abedin S, Borissenko N, Endres F. Electrochem Commun 2004;6(4):422–6.

[9] (a) Innis PC, Mazurkiewicz J, Nguyen T, Wallace GG, Macfarlane D. Curr Appl Phys 2004;4(2–4):389–93;
(b) Li MC, Ma CA, Liu BY, Jin ZM. Electrochem Commun 2005;7(2): 209–12.

[10] (a) Randriamahazaka H, Plesse C, Teyssié D, Chevrot C. Electrochem Commun 2003;5(7):613–7;
(b) Randriamahazaka H, Plesse C, Teyssié D, Chevrot C. Electrochem Commun 2004;6(3):299–305;
(c) Damlin P, Kvarnstrm C, Ivaska AJ. Electroanal Chem 2004;570(1): 113–22.

[11] Xu JK, Liu HT, Pu SZ, Li FY, Luo MB. Macromolecules 2006;39(17): 5611–6.

[12] Dupont J, Consorti CS, Suarez PAZ, de Souza RF, Fulmer SL, Richardson DP, et al. Org Synth 2002;79:236–40.

[13] Zimmermann C, Mohr M, Zipse H, Eichberger R, Schnabel W. J Photochem Photobiol A Chem 1999;125(1–3):47–56.

[14] Tasi FC, Chang CC, Liu CL, Chen WC, Jenekhe SA. Macromolecules 2005;38(5):1958–66.

[15] Otero TF, de Larreta-Azelain E. Polymer 1988;29(8):1522–7.

[16] (a) Shi GQ, Xu JK, Fu MX. J Phys Chem B 2002;106(2):288–92;
(b) Fu MX, Shi GQ, Chen FE, Hong XY. Phys Chem Chem Phys 2002;4(12):2685–90;

(c) Xu JK, Zhou WQ, Hou J, Pu SZ, Yan LS, Wang JW. J Polym Sci Part A Polym Chem 2005;43(17):3986–97.

[17] Zhou M, Heinze J. Electrochim Acta 1999;44(11):1733–48.

[18] (a) Pommerehne J, Vestweber H, Guss W, Mahrt RF, Bassler H, Porsch M, et al. Adv Mater 1995;7(6):551–4;
(b) Zhan XW, Liu YQ, Wu X, Wang S, Zhu DB. Macromolecules 2002;35(7):2529–37;
(c) Li HC, Lambert C, Stahl R. Macromolecules 2006;39(6):2049–55.

[19] Sak-Bisnar M, Budimir M, Kovac S, Kukulj D, Duic L. J Polym Sci Part A Polym Chem 1992;30(8):1609–14.

[20] Thiéblemont JC, Brun A, Marty J, Planche MF, Calo P. Polymer 1995;36(8):1605–10.

[21] Bock C, Smith A, MacDougall B. Electrochim Acta 2002;48(1):57–67.

[22] Ohno H. Electrochemical aspects of ionic liquids. Hoboken, New Jersey: John Wiley & Sons, Inc.; 2005.

[23] Cho SI, Kwon WJ, Choi SJ, Kim P, Park SA, Kim J, et al. Adv Mater 2005;17(2):171–5.